PRESSURE-INDUCED AMORPHIZATION IN PLAGIOCLASE FELDSPAR: A TIME-RESOLVED POWDER DIFFRACTION STUDY DURING RAPID COMPRESSION. M. Sims[1], S.J. Jaret[1], E. Carl[2], B. Rhymer[1], N. Schrodt[3], V. Mohrholz[4], J. Smith[5], Z. Konopkova[6,7], H.P. Liermann[6], T.D. Glotch[1] and L. Ehm[1,8], [1]Stony Brook University, Stony Brook, NY 11794-2100, USA (melissa.sims@stonybrook.edu), [2]University Freiburg, D-79098 Freiburg, Germany, [3]Goethe-University Frankfurt, D-60438 Frankfurt, Germany, [4]Friedrich Schiller University Jena, D-07737 Jena, Germany, [5]High Pressure Collaborative Access Team, Carnegie Institution of Washington, Argonne, Il 60439, USA, [6]Photon Sciences, Deutsches Elektronen Synchrotron, D-22607 Hamburg, Germany, ,[7]European XFEL GmbH, Holzkoppel 4, 22869 Schenefeld, Germany, [8]National Synchrotron Light Source II, Brookhaven National Laboratory, Upton, NY11973, USA

Introduction: Impact cratering is important in planetary body formation and evolution [1, 2]. The pressure and temperature conditions during impacts are classified using systems [3] that stem from 1) petrographic features observed in the impactite and 2) the presence of high pressure mineral phases. Plagioclase ((Na_{1-x} Ca_x)Al_{1+x} Si_{2-x} O_8) is used in these systems because it is common on rocky bodies throughout the Solar System. Maskelynite, amorphous plagioclase, forms in the range between 25 and 45 GPa [4] and is used as an indicator of petrographic type S5 (strongly shocked). However, the formation pressure of maskelynite is uncertain because different experimental techniques produce it at different pressures [5,6].

Formation pressures of impact-generated mineral phases are determined using experiments that involve static or dynamic pressure generation. These experiments have different strain rates and timescales of completion compared to natural impact events. In addition, static and shock experiments follow different pressure-temperature paths than natural impacts [7,8].

Shock experiments produce amorphization at pressures > 10 GPa higher than static diamond anvil cell (DAC) experiments [8]. The difference cannot be attributed to the greater temperatures during shock experiments because amorphization pressure decreases with increasing temperature [8-10]. Kinetics or strain rate may play a role in this process. Huffman and Reimold [10] propose that amorphization onset pressure is a function of applied strain rate and total work done. The total work done must be sufficient to initiate amorphization, so static experiments may not generate the lowest formation pressure possible. We test these hypotheses in order to relate our observations to a formation mechanism of maskelynite.

Samples and Methods: We utilize rapid compression, in order to study the effect of strain rate on plagioclase amorphization pressure. Natural anorthite (Grass Valley, Ca) and albite (Amelia County, Va) were compressed to 80 GPa at multiple rates recorded in a total of 16 experiments. Symmetric-type diamond anvil cells were used for pressure generation. Gold and NaCl were used as internal pressure standards. Samples were compressed without a pressure medium. Compression rate in the experiments was controlled in the DAC by either the inflation a membrane (mDAC) [11] or extension of piezoelectric actuator (dDAC) [12].

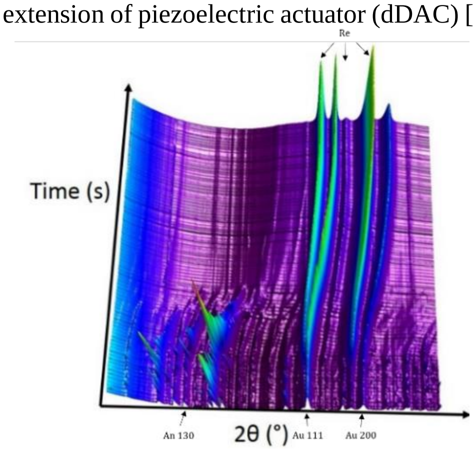

Fig. 1: 3D plot of ambient temperature rapid compression of anorthite data consisting of a series of integrated 1D X-ray diffraction patterns. Pressure increases in time on the Y-axis at 0.2 GPa/s. Arrows identify individual peaks from the sample (An 130), pressure standard (Au) and gasket (Re).

The setup creates strain rates of 10^{-3} s^{-1} with compression ranging from minimum rates of 0.02-1 GPa/s (mDAC) up to 15-80 GPa/s (dDAC). High-pressure experiments were conducted at the Extreme Conditions Beamline (ECB) at PETRA-III at DESY, Germany and the HPCAT beamline 16-IDB at the Advanced Photon Source (APS) at Argonne National Laboratory, USA.

Time-resolved X-ray powder diffraction patterns were collected during compression, holding and decompression cycles. Diffraction patterns were taken every 0.1, 0.5, or 1 second depending on the compression rate. The diffraction images were recorded on a Perkin-Elmer XRD 1621 flat panel detector using 0.4847 Å X-rays at the ECB at PETRA III. At 16-ID-B at APS, the patterns were collected on a DECTRIS Pilatus 1M detector using X-rays with a wavelength of

0.6199 Å. In order to ensure sufficient time resolution during the experiments utilizing the dDAC at the ECB, a GaAs LAMBDA detector from X-Spectrum was employed. The geometric parameters for the reduction of the 2D diffraction images were determined from a CeO_2 standard and the radial integration of the two-dimensional data was performed with DIOPTAS [13].

Amorphization was considered to be completed when diffraction peaks became indistinguishable from background intensity. We used LeBail analysis [14] to determine changes in lattice parameters with pressure. The calculated lattice parameters were then used to determine a Birch-Murnaghan equation of state and to calculate volume strain, resulting in plots of stress (pressure) and volume strain as function of pressure.

Recovered samples were imaged on a LEO 1550 field emission scanning electron microscope (SEN) instrument at 2.5 kV at Stony Brook University.

Results:

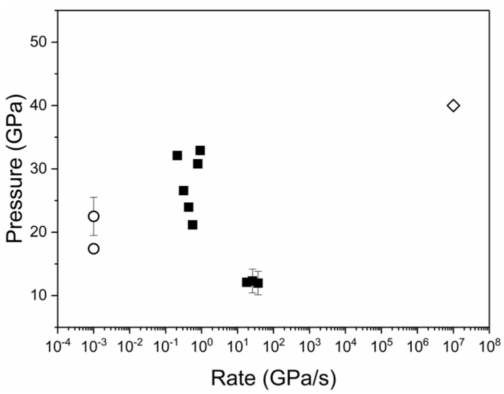

Fig.2: Anorthite total amorphization pressure vs. compression rate data. Circles are static values [5, 15] squares are from this work, and the diamond is a shock value [6].

We find an overall decrease in amorphization completion pressure with increasing compression rate for both datasets (Fig 2). In albite dDAC data, the trend of amorphization completion pressure is not as clear as in the anorthite dDAC dataset. Static DAC values are considered to take place over the course of an hour, but represent fast compression with long rest periods. Additional measurements would be useful for verification of the trends. Based on our equation of state calculations, we observe a decrease in bulk moduli with increasing rate for the albite data. The trend in stress-volume strain calculations suggests albite becomes more ductile with increasing compression rate. Overall, the equation of state and stress-strain calculations indicate albite becomes softer and more plastic with increasing compression rate.

The SEM images (Fig. 3) demonstrate a change in microstructure that is compression-rate related. The grain size of the recovered samples generally becomes finer with increasing compression rate. The sample from the 0.1(5) GPa/s run (b) shows a homogeneous distribution of nanocrystalline grains, while the 35(4) GPa/s run has a more heterogeneous grain size and morphology (c).

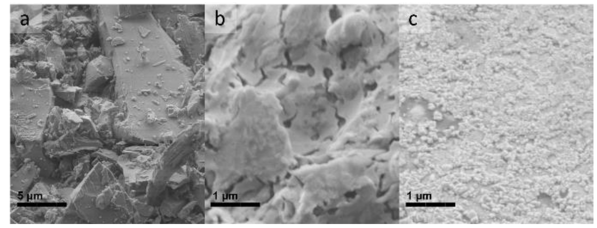

Fig. 3: SEM images of three albite samples. a. is the albite sample before experimentation, b is the recovered sample from the 0.1(5) GPa/s run, and c. is the recovered sample from the 35(4) GPa/s runs.

Discussion: The overall reduction in amorphization pressure with compression rate is indicative of negative strain rate sensitivity (SRS). Negative SRS is consistent with models suggested by Huffman and Reimold [10]. Their model is based on 'shear-melting' theory from Grady [16]. Grady's theory proposes intrinsic instabilities in the thermomechanical deformation process cause deformation to be localized into thin planar regions. Negative SRS implies shear deformation occurs and is localized. Grady also predicts a reduction in strength with increasing compression rate that we observe as increased plasticity and a decrease in bulk moduli. Our data suggests shock-induced differential stress may not be necessary for shear deformation.

We demonstrate correlation between deformation modes and strain rates. Since the amorphization pressure depends on compression rate, careful usage of amorphization as an impact barometer may be required.

References: [1] French B.M. and Short N.M., Shock Metamorphism of Natural Materials. [2] Melosh H.J. (1989) Impact Cratering. A Geologic Process. [3] Stöffler et al. (1991) GCA., 55, 3845-3867. [4] Chao E.C.T. (1968) In Shock Metamorphism of Natural Materials, 135. [5] Daniel I. et al. (1997) JGR: Solid Earth, *102*, *B5*, *10313-10325*. [6] Velde B. (1989) Phys. Chem. Miner., *16*, 5, 436-441. [7] Ahrens T. (1969) JGR, *74*, 2727-2746. [8] Tomioka N. et al. (2010) GRL, *37*, 1-5. [9] Langenhorst F. and Deutsch A. (1994) EPSL, *128*, 683-698. [10] Huffman A.R. and Reimold W.U. (1996) Tectonophysics. *256*, 165-217. [11] Letoullec R. et al. (1988) HPR. *1*, 77-90. [12] Evans W.J. et al. (2007) Rev. Sci. Instrum., *78*, 073904. [13] Prescher C. and Prakapenka V. (2015) High Pressure Res., *35*, 3, 223-230. [14] LeBail A. (2005) Powder Diffr. *20*, 316. [15] Redfern S. (1996) Min. Mag., *60*, 493-498. [16] Grady D. (1980) JGR: Solid Earth, *85*, *B2*, 913-924.